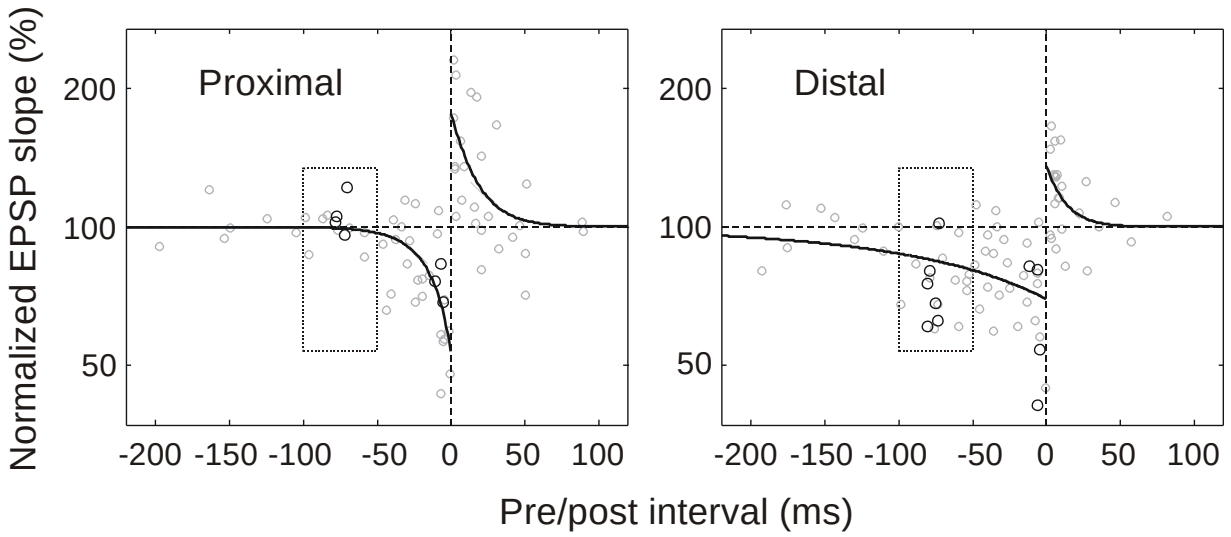

Supplementary Figure 1. Spike-timing-dependent synaptic depression at proximal and distal dendrites in the presence of 10 μM picrotoxin (black circles), superimposed on the STDP window measured in normal bath solution (gray circles, same as Fig. 1d). At $-100<\Delta t<-50$ ms, significant LTD was induced at distal (–25.2±6.1%, n=6, $p<0.01$) but not at proximal dendrite (6.8±5.6%, n=4, $p>0.8$).

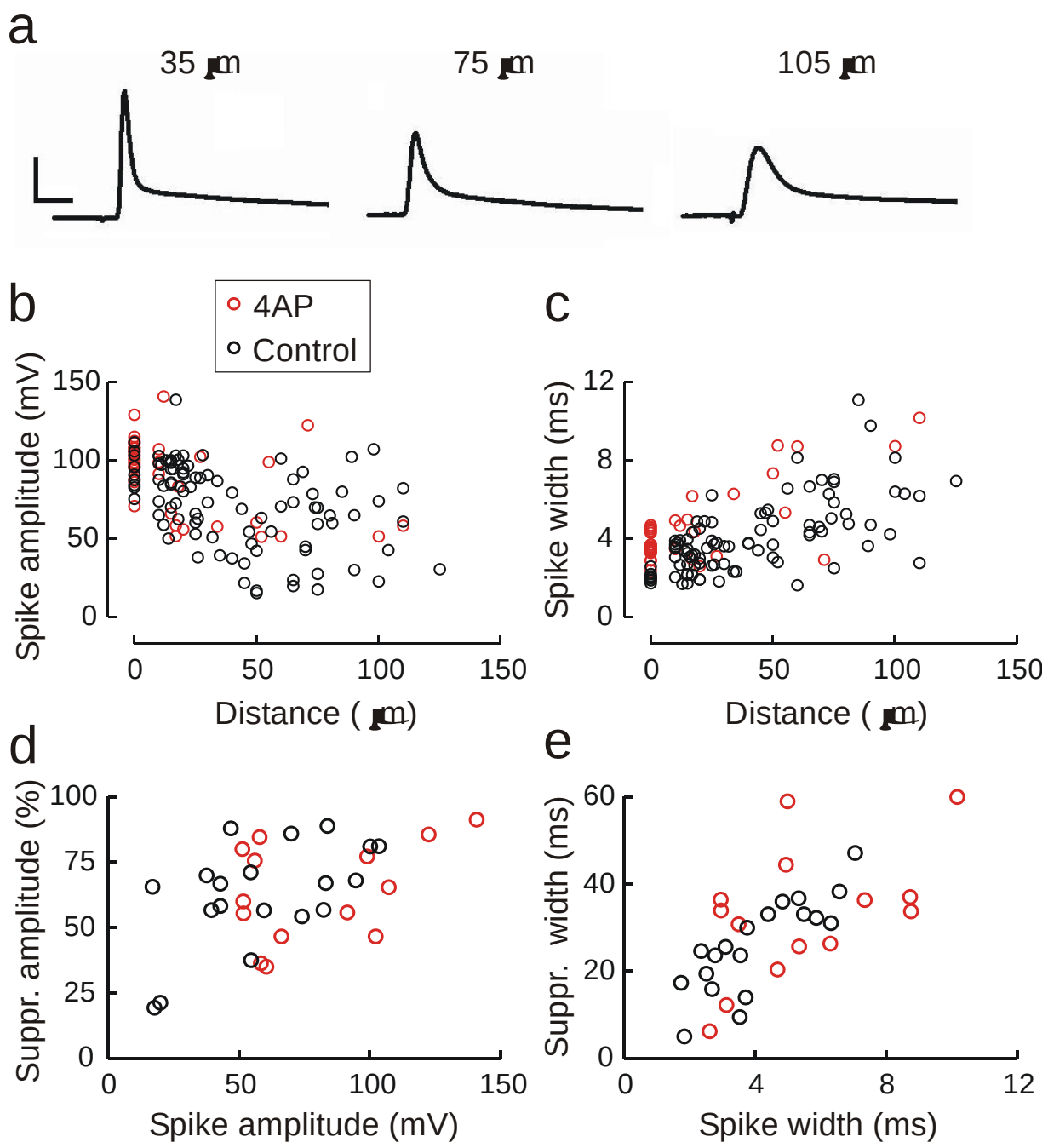

Supplementary Figure 2. Back-propagating APs and AP-induced suppression of EPSPs recorded from apical dendrites of L2/3 pyramidal cells. **a**, Examples of back-propagating APs recorded at 35, 75, and 105 μm from the soma (from different cells). APs were evoked antidromically with a small stimulating electrode placed at the axon initial segment. Scale bars: 40 mV, 5 ms. **b**, Spike amplitude as a function of dendritic distance from the soma. Red symbols indicate experiments performed with 4-AP (3 mM) in the recording electrode. **c**, Spike width (measured at half-height of the AP) as a function of dendritic distance. **d**, Amplitude of EPSP suppression window as a function of spike amplitude. Each suppression window was fit with a single exponential $1-Ae^{-t/\tau}$; A is used to represent amplitude. **e**, Width of EPSP suppression window (measured at half-height of the exponential fit, which equals $\tau \log 2$) as a function of spike width.

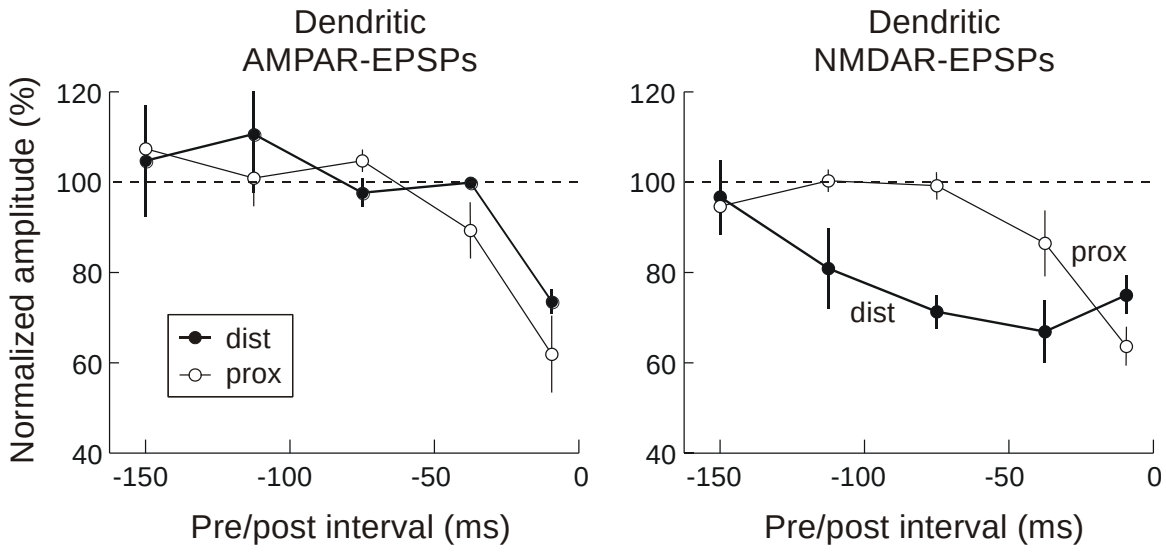

Supplementary Figure 3. Suppression of AMPAR-EPSP and NMDAR-EPSP by back-propagating AP. Same as Fig. 2e, f, except that the recordings were made in the dendrite near the stimulating electrode. n=2 to 6 (AMPAR-EPSPs) and 3 to 7 (NMDAR-EPSPs).

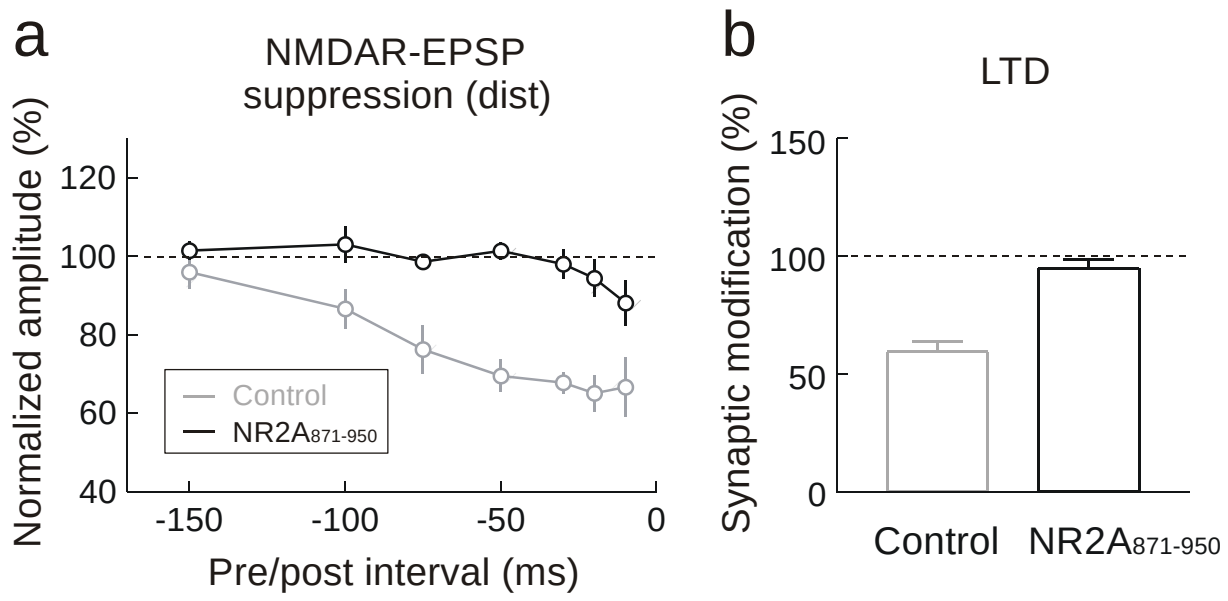

Supplementary Figure 4. Expression of $NR2A_{871\text{-}950}$ blocks NMDAR-EPSP suppression and LTD induction. **a**, Temporal windows of AP-induced suppression of NMDAR-EPSPs at distal dendrite of infected (black line, n=4) and control (gray line, n=7 to 12) L2/3 pyramidal neurons. Error bar: ± s.e.m. Data were significantly different over the following pre/post intervals: –10 ms ($p<0.05$), –20 ms ($p<0.01$), –30 ms ($p<0.001$), –50 ms ($p<10^{-6}$), –75 ms ($p<0.01$), and –100 ms ($p<0.05$); *t* test. **b**, LTD was induced by 60 post→pre spike pairs for control (–40.4±4.3%; n=18) but not for infected neurons (–5.1±3.9%; n=3; $p>0.4$, *t* test). The difference between control and infected cells was significant ($p<0.001$, *t* test).

Methods. Using standard molecular biology techniques, GFP was inserted before a sequence corresponding to residues 871-950 of the NR2A subunit of the NMDAR, a serine-containing region of the C-terminus important for calcineurin-dependent NMDAR desensitization (Krupp et al., 2002, *Neuropharmacology* **42**:593). Semliki Forest Virus (SFV) containing this construct was made by co-transfecting HEK293 cells with pSCA3-GFP-NR2A and pSCAhelper using lipofectamine 2000. After 48 hours, culture media was harvested and virus was activated with 0.5mg/ml α-chymotrypsin (45 min, room temperature). Surgeries were performed in 4-week old rats in accordance with the guidelines of the Animal Care and Use Committee at the University of California, Berkeley. Rats were anesthetized with ketamine (80 mg/kg) and xylazine (10 mg/kg). Small craniotomies (1 mm^2) were performed over the visual cortex and SFV-containing media was injected into the superficial cortex with a small pipette (15 μm tip diameter). Rats were allowed to recover for two days before brain slices were cut (Takahashi et al., 2003, *Science* **299**:1585). Infected cells were identified based on GFP labeling. Resting membrane potentials and input resistance of infected neurons were not significantly different from age-matched control neurons ($p>0.3$).

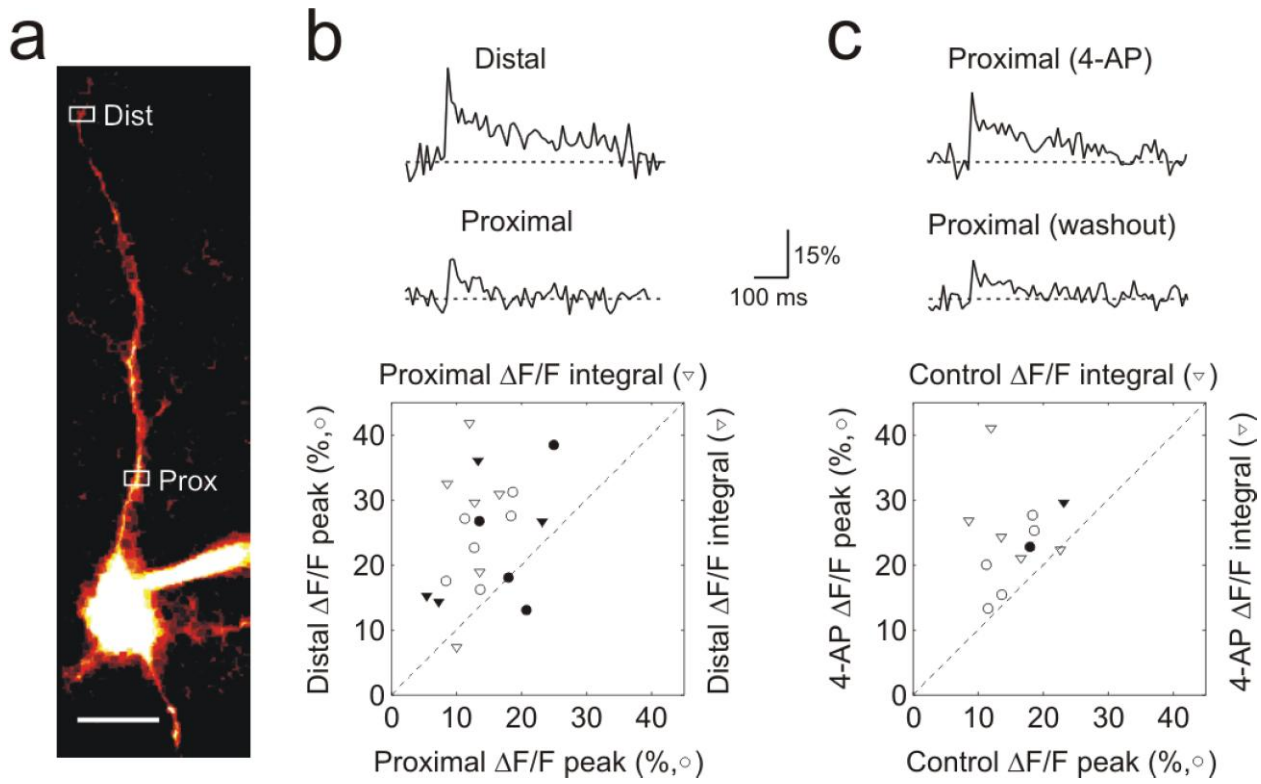

Supplementary Figure 5. Dendritic Ca^{2+} signal evoked by back-propagating AP. **a**, Two-photon fluorescence image of a layer 2/3 pyramidal neuron filled with 200 μM Oregon Green BAPTA 1. Scale bar: 20 μm. **b**, *Upper traces*: Fluorescence Ca^{2+} signals at distal (108 μm) and proximal (22 μm) dendrites (white boxes in **a**) in response to single back-propagating APs evoked by somatic current injection, each averaged from 11 to 18 trials. *Lower plot*: distal vs. proximal Ca^{2+} signals evoked by single APs, measured by either peak amplitude (○) or peak area (integral, ▽, in arbitrary units). Each symbol represents data from one cell (n=10); open symbol: with 100 μM Oregon Green BAPTA 1; filled symbol: 200 μM. **c**, 4-AP enhances the AP-induced Ca^{2+} signal at proximal dendrite. *Upper traces*: Ca^{2+} signals at proximal dendrite of the cell shown in (**a**) in the presence of extracellular 4-AP and after washout. *Lower plot*: AP-induced Ca^{2+} signals at proximal dendrite after vs. before bath application of 4-AP (n=6).

Method. Oregon Green BAPTA 1 (100-200 μM, Molecular Probes) was loaded into the cell via the somatic whole-cell pipette (loading time before imaging: ~15 min). Imaging was done using a two-photon laser scanning system consisting of an upright microscope (DM LFS, Leica Microsystems, Heidelberg) with 40×W0.8IR objective and a "Tsunami" titanium-sapphire laser pumped by a "Millennia" neodymium yttrium vanadate solid state laser (SpectraPhysics, Mountain View, CA), which provides <100 fs pulses at 890 nm at 80 MHz. Line-scan mode was used to record single AP-induced Ca^{2+} transients (temporal resolution: 1 ms). At each dendritic location, 5 to 71 sweeps were measured (interleaved between distal and proximal sites), and results were averaged. Change in Ca^{2+} concentration is given in the change of fluorescence normalized by baseline fluorescence (ΔF/F) after background correction. Data were analyzed in Matlab (MathWorks).

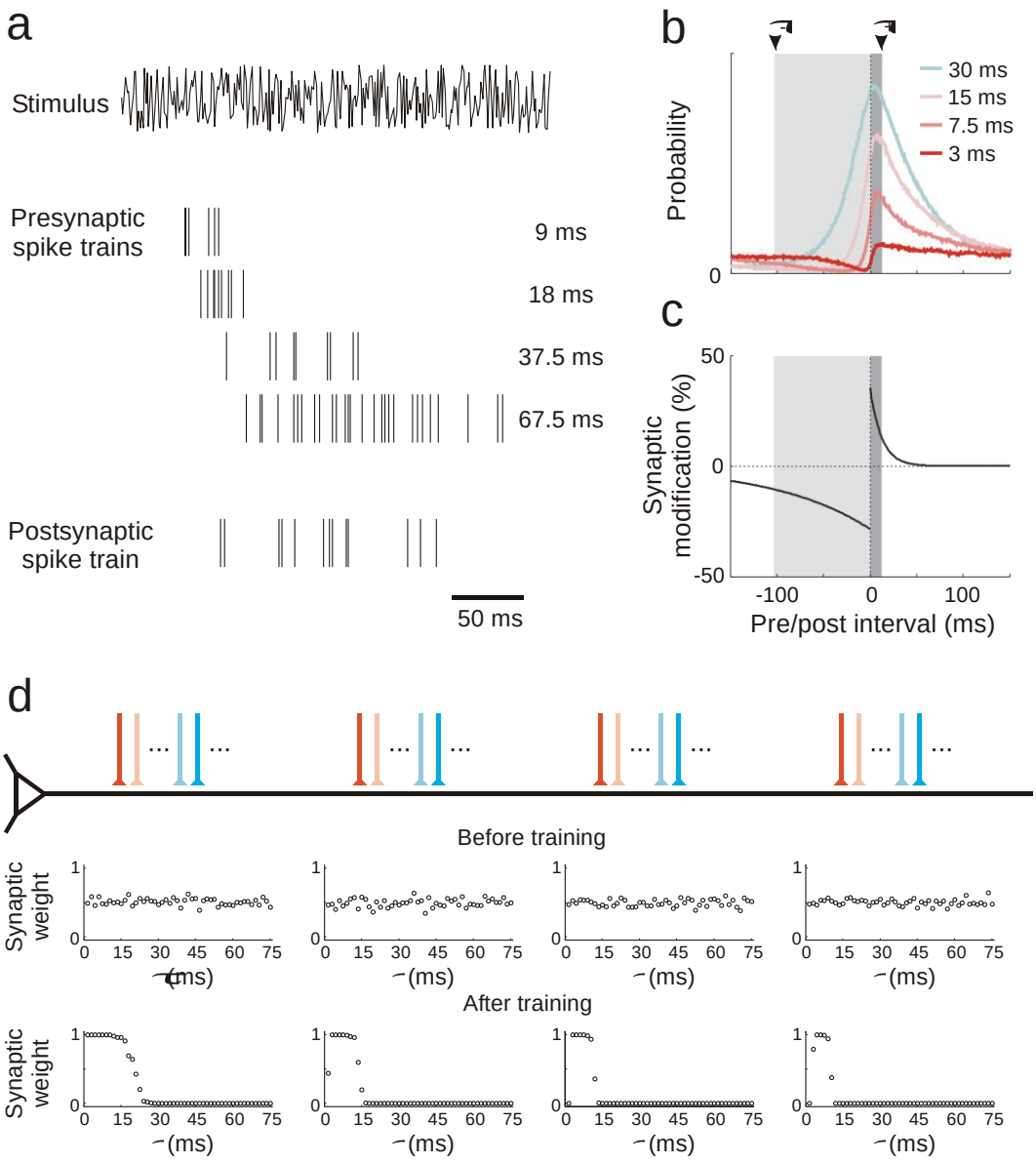

Supplementary Figure 6. Further analyses of the model on location-dependent input selection. **a**, Sensory stimulus used in simulation and spike trains of example model neurons. Number on the right of each presynaptic spike train indicates time constant of impulse response function of the cell (τ_i, see Supplementary Methods). To effectively illustrate the relative spike timing, spike trains are shown for a selected period with high-frequency bursts from many presynaptic neurons; the overall mean firing rate of the cells were much lower. **b**, Cross-correlogram between pre- and postsynaptic spike trains. Warmer colors represent inputs with more transient responses (numbers on the right indicate τ_i). The number of pre/post spike pairs contributing to LTP and LTD can be roughly estimated from the dark and light shaded areas under each curve; dark shading: width of LTP window in **c** (τ_+=12.5 ms), light shading: width of LTD window (τ_-=103.4 ms). **c**, Single exponential fit of the STDP window measured at distal dendrites. **d**, Simulation results of a 4-compartment model. Shown are diagram of synaptic inputs (upper), and synaptic weight vs. τ_i before (middle) and after (lower) training. The location dependence of input selection is similar to that found in the 2-compartment model (Fig. 5b).